Department of Human Anatomy, Histology and Embryology[1], College of Basic Medicine; Department of Immunology[2], College of Basic Medicine, Jiamusi University, Jiamusi, China; Department of Pediatrics[3], Mbeya Zonal Referral Hospital, Tanzania

Hexarelin protects cardiac H9C2 cells from angiotensin II-induced hypertrophy *via* the regulation of autophagy

E. Agbo[1], M-X. Li[1], Y-Q. Wang[1], R-O. Saahene[2], J. Massaro[3], G-Z. Tian[1,*]

Received January 14, 2019, accepted February 15, 2019

**Corresponding author: GuoZhong Tian, PhD, College of Basic Medicine, Department of Human Anatomy, Histology and Embryology, Jiamusi University, No. 148 Xuefu Street, Jiamusi 154007, P. R. China 858459001@qq.com*

Pharmazie 74: 485-491 (2019) *doi: 10.1691/ph.2019.9324*

Hexarelin is a synthetic growth hormone-releasing peptide that exerts cardioprotective effects. Regulation of autophagy is known to be cardioprotective so this study examined the role of autophagy and potential regulatory mechanisms in hexarelin-elicited anti-cardiac hypertrophic action in cardiomyocytes subjected to hypertrophy. H9C2 cardiomyocytes were subjected to hypertrophy by angiotensin-II (Ang-II). Autophagic light chain-3 (LC3) and cytoskeletal proteins were determined by immunofluorescence assay. Autophagy was also detected using monodansylcadaverine (MDC) for autophagic vacuole visualization and Cyto-ID staining for autophagic flux measurement. Molecular changes were analysed by Western blotting and qRT-PCR. Apoptosis was evaluated using flow cytometry and TUNEL assay. ATP content and CCK-8 assay were used in assessing enhanced cell survival whilst oxidative stress was analysed by measuring malondialdehyde(MDA) and superoxide dismutase(SOD) levels. Ang-II induced cardiomyocyte hypertrophy, oxidative stress, apoptosis and decreased cell survival, all of which were significantly suppressed by hexarelin treatment which also enhanced autophagy in hypertrophic H9C2 cells. Furthermore, inhibition of hexarelin induced autophagy by 3-methyladenine (3MA) abolished the anti-hypertrophic function of hexarelin and also abrogated the protection of hexarelin against cell survival inhibition and apoptosis. Conversely, the application of autophagy stimulator rapamycin in H9C2 hypertrophic cells inhibited apoptosis, cell survival and reduced cell size as well. Additionally, hexarelin regulated the upstream signalling of autophagy by inhibiting the phosphorylation of mammalian target of rapamycin(mTOR). We propose that hexarelin plays a novel role of attenuating cardiomyocyte hypertrophy and apoptosis *via* an autophagy-dependent mechanism associated with the suppression of the mTOR signalling pathway.

1. Introduction

Heart failure (HF), simply described as a decline in the heart's adequate blood pumping ability to meet the requirements of the body (Mudd and Kass 2008), is regarded as one of the greatest challenges in the medicine of the cardiovascular system and considered as having a prognosis worse than that of most cancers (Stewart et al. 2001). Pathological cardiac hypertrophy, identified as a leading predictor of HF (Okin et al. 2007), refers to the persistent enlargement of the cardiac muscles, occurring as a response to cardiac injuries like myocardial infarction and hypertension (Hill and Olson 2008). It is characterised at the cellular level by the increase in the size of cardiomyocytes, protein synthesis, alterations in gene expression and organization of sarcomeres (Bisping et al. 2014; Hill and Olson 2008). Numerous cardiac hypertrophic signalling pathways responsible for triggering cardiac hypertrophy has been shown to be activated by several factors such as stress releasing hormones, cytokines, growth factors and biomechanical stress stimuli (Heineke and Molkentin 2006). In fact, the independent risk factor of HF from a data of human subjects in 2011 was revealed to be left ventricular hypertrophy, hence mortality is reduced when left ventricular mass is decreased (Koitabashi and Kass 2012). These therefore point to the fact that preventing and reversing cardiac hypertrophy must be a prime objective for any therapeutic advancement for the prevention or cure of HF. Modern treatments of HF such as angiotensin converting enzyme (ACE)-inhibitors as well as β-blockers improve cardiac hypertrophy by reducing the heart rate and hemodynamic load, which reduces the stress stimulus for cardiomyocyte growth (Katz 2008). Unfortunately, the progression of HF still persists, recording high mortality rates (Bisping et al. 2014) and therefore more targeted approaches to attenuating maladaptive hypertrophy are desired.

Autophagy is a process that involves lipid and protein bulk recycling and degradation in organisms and in mammals as well. Cell development and growth, turnover and biogenesis of organelles are all critical roles played by autophagy (Mizushima and Komatsu 2011). According to recent studies, the enhancement of autophagy in the myocardium offers cardioprotection whilst the inhibition of autophagy is associated with the development of cardiac hypertrophy and HF (Orogo and Gustafsson 2015; Wu et al. 2014) . For example, the loss of ATG5, a protein related to autophagy, results in cardiac hypertrophy (Nakai et al. 2007). Ang-II is shown by several studies to induce cardiac hypertrophy but its mechanism of action still remains to be fully understood especially with respect to its effect on autophagy. Several studies have emphasized that apoptosis is associated with cardiac hypertrophy and the progression to HF but recent investigations have also implicated the involvement of autophagy related to the pathogenesis of cardiomyocyte apoptosis and cardiac hypertrophy (Gottlieb and Mentzer 2010; Li et al. 2017).

Ghrelin, a known growth hormone secretagogue (GHS) secreted in the stomach, is an endogenous ligand of GHS receptor-1a (GHSR1a) with numerous cardioprotective actions. Studies have also shown autophagy regulatory actions of ghrelin in a variety of tissues (Rodriguez et al. 2012; Yuan et al. 2014) and notable among them is a study by Tong et al. (2012), which showed the cardioprotective activity

of ghrelin against cardiac myocyte injury by inducing autophagy. Hexarelin, a synthetic mimetic of ghrelin, is a synthetic growth hormone-releasing peptide that binds to both GHSR1a and the cardiac non-GHS receptor CD36 to exert its cardioprotective effects (Mao et al. 2013). As proved by several studies, the existence of both receptors is indicative of hexarelin's direct cardiovascular actions independent of the release of growth hormone and neuroendocrine stimulation (Mao et al. 2014). Hexarelin is capable of exerting cardioprotective effects like the prevention of cardiomyocyte apoptosis (Filigheddu et al. 2001), atherosclerosis (De Gennaro-Colonna et al. 2000) and cardiac fibrosis (Xu et al. 2007). However, its cardioprotective effects and mechanism against cardiac hypertrophy with respect to autophagy regulation is yet to be reported.

In this current study, we employed the use of a model of angiotensin II-induced hypertrophy in embryonic rat heart-derived cardiomyocyte H9C2 cell line to investigate the anti-cardiac hypertrophic effect and potential regulatory mechanisms of hexarelin with respect to autophagy regulation, and we further explored the interactive relationship between apoptosis and hexarelin-elicited autophagy in the angiotensin II-induced hypertrophic H9C2 cell line model.

2. Investigations and results

2.1. Effect of Ang-II and hexarelin on the cell viability of H9C2 cells

For the identification of the best concentration and treatment time of Ang-II for our study, H9C2 cardiomyocytes underwent treatment with different concentrations (0 to 10 μM) at different times (0 to 48 h) and the cell viability were determined by CCK-8 assay. Figure 1A shows that, compared with the control group, although 0.5 μM of Ang-II significantly (P<0.01) reduce cell viability (89.88±0.74) already, treatment with 1 μM of Ang-II caused a much more significant (P<0.0001) decrease in cell viability (72.22±2.42) and at the best treatment time of 24 h which also demonstrates the time dependency of the effect of Ang-II (Fig.1B). Cell survival of H9C2 cells were not affected by hexarelin treatment alone (Fig.1C) but 1 μM hexarelin treatment of H9C2 cells at 24 h was enough to attenuate Ang-II-induced cell death (Fig. 1D). We subsequently used 1 μM of Ang-II and hexarelin at 24 h for the rest of our study.

2.2. Hexarelin inhibits angiotensin-II induced hypertrophy in H9C2 cardiomyocytes

The effect of hexarelin on Ang-II-induced myocardial cell hypertrophy was investigated and hypertrophy was evaluated by the detection of an increase in cell surface area by immunofluorescence for cardiac α-actin. Fig. 2A and 2B showed that, compared to the control group, Ang-II significantly increased (p< 0.05) the cell surface area of H9C2 cells whilst hexarelin significantly attenuated this increase when Ang-II+Hex group was compared to the Ang-II group. Further evaluation of the hypertrophic markers BNP and ANP by western blotting or PCR (Fig. 2C, 2D and 2E) showed that, Ang-II increased the protein and mRNA expressions of BNP significantly (p< 0.05) and also showed a significant increase (p< 0.05) in the mRNA expression of ANP (Fig. 2D). Hexarelin significantly (p< 0.05) reversed all these increases to confirm that hexarelin indeed inhibits angiotensin-II induced hypertrophy in H9C2 cells. It is worth noting that the effects of hexarelin were consistent with that of rapamycin (a classical autophagy inducer) when Ang-II+Hex group and Ang-II+RAPA group were compared to the Ang-II group. Another interesting observation was that, a comparison between Ang-II + Hex and Ang-II + Hex + 3-MA groups showed that 3-MA (a classical autophagy inhibitor) significantly (p< 0.05) abrogated all the effects of hexarelin and hence increased the cell surface area and BNP protein expression of the H9C2 cells.

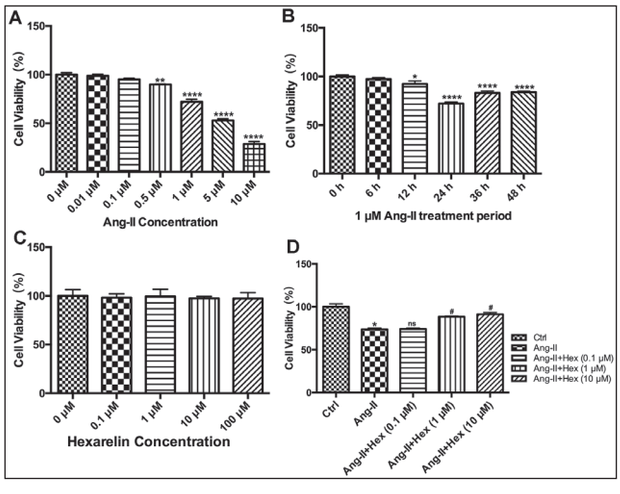

Fig. 1: Effect of Ang-II and hexarelin on the cell viability of H9C2 cells. Cell viability was determined by CCK-8 analysis after treatment of H9C2 cells with: (A) different concentrations of Ang-II for 24 h, (B) 1 μM Ang-II from 0 h to 48 h, (C) different concentrations of hexarelin at 24 h, and (D) 1 μM Ang-II and different concentrations of hexarelin at 24 h. ns = no significance, * P<0.05, ** P<0.01, **** P<0.0001 versus control group (0 μM group, 0 h group or Ctrl group); #P<0.05 versus Ang-II group (n=8).

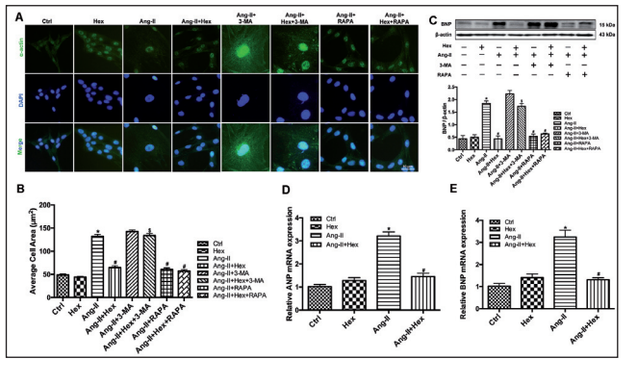

Fig. 2: Hexarelin inhibits Ang-II induced hypertrophy in H9C2 cardiomyocytes. (A) Representative images of cytoskeletal proteins in H9C2 cells after the various group treatments. Scale bar=10 μm. (B) Quantification of changes in H9C2 cell surface area after the various group treatments using Image J software (n=6). (C) Representative Western blotting images and quantitative results showing the protein expression level of BNP in H9C2 cells after the various group treatments (n=3). (D and E) Representative qRT-PCR analysis of mRNA expression levels of ANP and BNP in H9C2 cells after the various group treatments (n=4). *P<0.05 versus Ctrl group; #P<0.05 versus Ang-II group; $P<0.05 versus Ang-II+Hex group.

2.3. Hexarelin increased the fluorescence intensity of autophagic LC3 protein in H9C2 cells

We monitored the induction of autophagy by analyzing the detection of microtubule-associated protein light chain 3 (LC3), which is a reliable autophagosome marker by immunofluorescence. As shown by our results (Fig. 3A), when compared to the Ctrl group, Ang-II markedly (p< 0.05) decreased the fluorescence intensity of LC3 protein but that effect was reversed by hexarelin treatment as indicated by the increase in fluorescence intensity of LC3 protein in the Ang-II + Hex group compared to the Ang-II group. This hexarelin effect was also consistent with the effect of rapamycin (a classical autophagy inducer) since rapamycin just like hexarelin also showed a significant increase (p< 0.05) in fluorescence intensity of LC3 as seen by comparing Ang-II + RAPA group to Ang-II group. A comparison between Ang-II + Hex and Ang-II + Hex + 3-MA groups revealed that, 3MA (a classical autophagy inhibitor) treatment diminished the hexarelin-induced increase in fluorescence intensity of LC3 protein. All these data suggest that hexarelin is capable of autophagy up-regulation in H9C2 cells.

2.4. Hexarelin increased the level of autophagosome formation in H9C2 cells

To further evaluate the autophagic effect of hexarelin in H9C2 cells, Cyto-ID® Green dye which is a fluorescent probe, was used

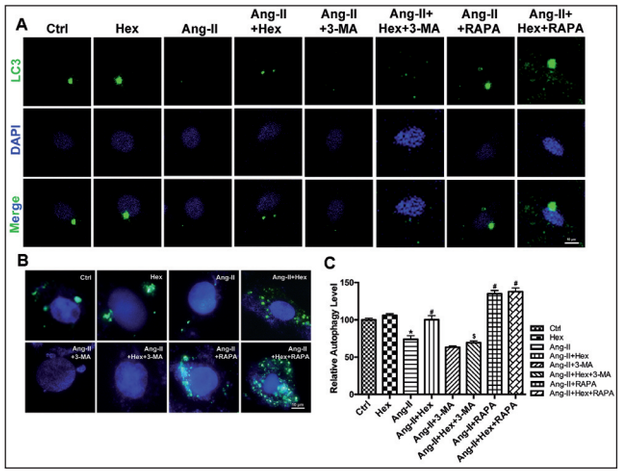

Fig. 3: Hexarelin increased LC3 protein fluorescence intensity and autophagosome formation in H9C2 cells. Representative Confocal Laser Scanning Microscopy (CLSM) images showing: (A) the expression of the autophagy marker protein LC3 in the various treatment groups of H9C2 cells (Scale bar=10μm) and (B) Cyto-ID® Green dye staining of autophagosomes in the various treatment groups (Scale bar=10μm). (C) Quantification results of the level of autophagy determined by the evaluation of the fluorescence intensity detected after Cyto-ID® Green dye staining of autophagosomes (n=5). *P<0.05 versus Ctrl group; #P<0.05 versus Ang-II group; $P<0.05 versus Ang-II+Hex group, (n=3).

in staining autophagosomes and the level of autophagy was determined and reflected by the evaluation of the fluorescence intensity detected. As shown by our results (Fig. 3B and 3C), when compared to the Ctrl group, Ang-II significantly ($p< 0.05$) decreased the fluorescence intensity of autophagosomes in the H9C2 cells but that effect was reversed by hexarelin treatment and consistent with the effect of rapamycin as indicated by the increase in fluorescence intensity of autophagosomes in the Ang-II + Hex and Ang-II + RAPA groups compared to the Ang-II group. However, 3-MA treatment abolished the hexarelin-induced increase in fluorescence intensity of autophagosomes as indicated by a comparison between Ang-II + Hex and Ang-II + Hex + 3-MA groups.

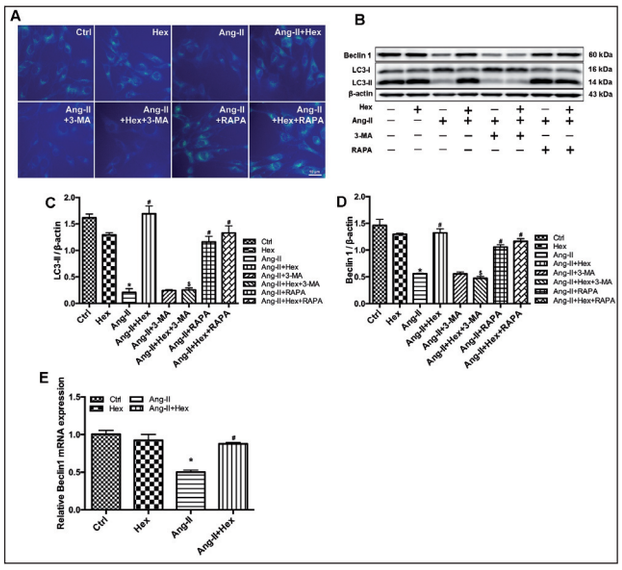

Fig. 4: Hexarelin increased autophagic vacuoles and LC3-II or Beclin-1 autophagic components in H9C2 cells. (A) Representative fluorescent microscopic images showing changes in MDC-positive autophagic vacuole formation in H9C2 cells after the various group treatments. Scale bar=10μm. (B, C and D) Representative Western blotting images and quantitative results showing the protein expression levels of LC3-II and Beclin-1 in H9C2 cells after the various group treatments (n=3). (E) Representative qRT-PCR analysis of mRNA expression level of Beclin-1 in H9C2 cells after the various group treatments (n=4). *P<0.05 versus Ctrl group; #P<0.05 versus Ang-II group; $P<0.05 versus Ang-II+Hex group.

2.5. Hexarelin increased MDC-positive autophagic vacuoles in H9C2 cells

Changes in autophagic activities were detected *via* the observation of MDC fluorescence, which has been identified to be a unique marker for autophagic vacuoles (Biederbick et al. 1995). Our results in Fig. 4A demonstrate that, hexarelin treatment in Ang-II + Hex group just like rapamycin, was capable of markedly increasing MDC-positive autophagic vacuoles that were initially decreased by Ang-II in the Ang-II group. 3-MA however, cancelled out the increase in MDC-positive autophagic vacuoles induced by hexarelin as made evident by comparing Ang-II + Hex group to Ang-II + Hex + 3-MA group.

2.6. Hexarelin upregulates protein or mRNA expressions of autophagy related LC3-II and Beclin1 in H9C2 cells

After H9C2 cells were treated with Ang-II, LC3-II and beclin-1 protein or mRNA expression patterns were investigated as shown in Fig. 4B, 4C, 4D and 4E. Ang-II significantly ($p< 0.05$) down-regulated beclin-1 and LC3-II protein expressions as well as the mRNA expression of beclin-1 in the H9C2 cells. Further treatment with hexarelin or rapamycin significantly ($p< 0.05$) abrogated the Ang-II induced inhibition of beclin-1 and LC3-II by up-regulating beclin-1 and LC3-II protein expressions in the H9C2 cells. The Ang-II induced inhibition of mRNA expression of beclin-1 was also significantly ($p< 0.05$) reversed upon hexarelin addition. Interestingly, 3-MA treatment abolished the hexarelin-induced upregulation of beclin-1 and LC3-II protein expressions as indicated by a comparison between Ang-II + Hex and Ang-II + Hex + 3-MA groups.

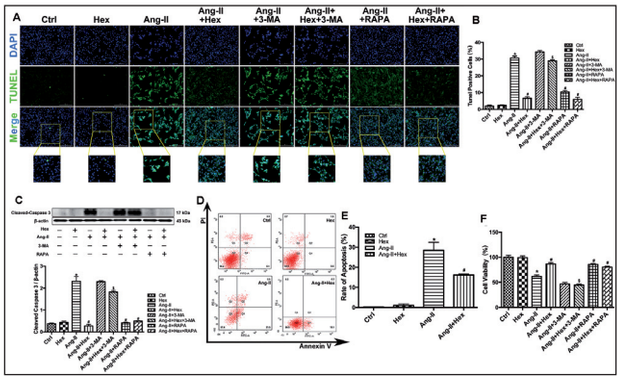

Fig. 5: Hexarelin-induced autophagy attenuated apoptosis induced by Ang-II. (A) Representative fluorescent microscopic images showing changes in TUNEL and nuclear staining in H9C2 cells after the various group treatments. Scale bar=200μm. (B) Quantification of apoptotic cells after TUNEL staining (n=3). (C) Representative Western blotting images and quantitative results showing the protein expression levels of cleaved caspase-3 in H9C2 cells after the various group treatments (n=3). (D) Representative graphs showing the evaluation of cell apoptosis by flow cytometry assay after Ctrl and Ang-II treated cells were incubated with hexarelin. (E) The statistical quantification of cell apoptosis in flow cytometry assay (n=3). (F) Determination of cell viability by CCK-8 analysis in H9C2 cells after the various group treatments (n=8). *P<0.05 versus Ctrl group; #P<0.05 versus Ang-II group; $P<0.05 versus Ang-II+Hex group.

2.7. Hexarelin-induced autophagy attenuated Ang-II-induced apoptosis in H9C2 cells

Our flow cytometry results (Fig. 5D and 5E) revealed that, compared to the Ctrl group, Ang-II significantly ($P < 0.05$) increased the rate of apoptosis of H9C2 cells. But hexarelin in Ang-II + Hex group significantly decreased ($P < 0.05$) the Ang-II induced increase in rate of apoptosis which suggests that hexarelin is capable of attenuating Ang-II induced apoptosis in H9C2 cells. To further confirm this, we performed TUNEL staining (Fig. 5A and 5B) of apoptotic H9C2 cells as well as Western blotting (Fig. 5C) to determine the protein expression pattern of cleaved-caspase 3. As expected, our Western blot and TUNEL staining results were consistent with

the flow cytometry results. There was a significant increase ($P < 0.05$) in cleaved-caspase 3 protein expression and TUNEL-positive H9C2 cells after incubation of H9C2 cells with Ang-II with the condensed and contracted appearance of some TUNEL-positive cardiomyocytes nuclei strongly suggesting apoptosis induced by Ang-II in H9C2 cells. Treatment of cells with both Ang-II and hexarelin significantly reduced ($P < 0.05$) cleaved-caspase 3 protein expression and TUNEL-positive H9C2 cells. Due to the known close association between autophagy and cell apoptosis, and considering the fact that hexarelin-induced autophagy in H9C2 cardiomyocytes in this present study, we used TUNEL staining and Western blot to find out whether hexarelin-induced autophagy was the main factor behind its apoptosis inhibition capability. We therefore employed the use of autophagy inhibitor and inducer, 3-MA and rapamycin respectively for this investigation. As shown by our results (Fig. 5A, 5B and 5C), when cells were treated together with Ang-II, hexarelin and 3-MA, the reduction in cleaved-caspase 3 protein expression and TUNEL-positive H9C2 cells caused by hexarelin seen in the Ang-II + hexarelin group were significantly abolished ($P < 0.05$) by 3-MA. This observation suggests that, the anti-apoptotic role of hexarelin depended on autophagy. Moreover, when we replaced hexarelin in Ang-II + Hex group with rapamycin (Ang-II + RAPA group) to induce autophagy, there were also significant reductions ($P < 0.05$) in cleaved-caspase 3 protein expression and TUNEL-positive H9C2 cells compared to the Ang-II group. This effect of rapamycin was very consistent with the effect of hexarelin which is made evident when Ang-II + Hex and Ang-II + RAPA groups were compared to the Ang-II group. All these observations suggest that hexarelin-induced autophagy was the main factor behind its apoptosis inhibition capability.

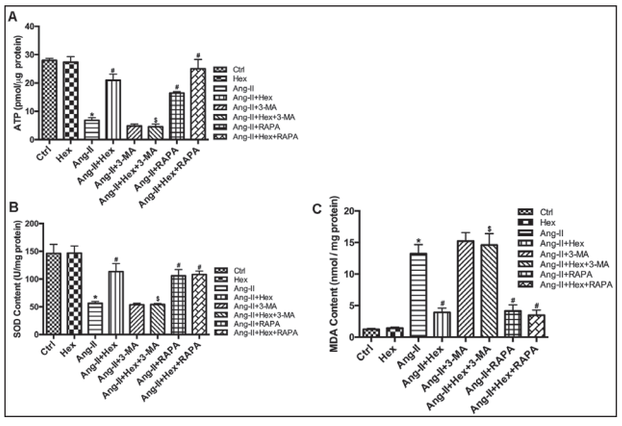

Fig. 6: Hexarelin-induced autophagy promotes cell survival by relieving oxidative stress and sustaining ATP production. (A) Representative graph showing the content of ATP measured by CellTiter-Glo® Luminescent Assay Kit in H9C2 cells after the various group treatments (n=3). (B) Representative graph showing the levels of SOD activity in H9C2 cells after the various group treatments (n=4). (C) Representative graph showing the content of MDA in H9C2 cells after the various group treatments (n=4). *P<0.05 versus Ctrl group; #P<0.05 versus Ang-II group; $P<0.05 versus Ang-II+Hex group.

2.8. Hexarelin-induced autophagy reversed Ang-II-induced depletion of cellular ATP and inhibition of cell viability in H9C2 cells

Fig. 5F and 6A showed that, compared to the control group, Ang-II significantly reduced ($p< 0.05$) the cell viability of H9C2 cells and markedly ($p< 0.05$) depleted H9C2 cellular ATP content. But hexarelin significantly ($p< 0.05$) reversed Ang-II induced depletion of cellular ATP and inhibition of cell viability in H9C2 cells when Ang-II+Hex group was compared to the Ang-II group. Rapamycin and 3-MA were then used to investigate hexarelin-induced autophagy's potential contribution to cell survival and cardioprotection. Interestingly, when autophagy was blocked with 3-MA in the Ang-II + Hex + 3-MA group, hexarelin's reversal of Ang-II induced depletion of cellular ATP and inhibition of cell viability in H9C2 cells were all abrogated proving that hexarelin-induced autophagy really enhanced cell survival. In addition, when Ang-II+Hex group and Ang-II+RAPA group were compared to the Ang-II group, we found out that the cardioprotective and cell survival enhancement effects of hexarelin were consistent with that of rapamycin.

2.9. Hexarelin-induced autophagy relieved the oxidative stress induced by Angiotensin-II in H9c2 cells

Compared to the Ctrl group, there was a significant increase ($p< 0.05$) in the MDA content (Fig. 6C) accompanied by a significant drop ($p< 0.05$) in the level of SOD (Fig. 6B) activity in the H9C2 cells that were incubated with Ang-II. Incubation of cells with both Ang-II and hexarelin markedly reversed ($p< 0.05$) the Ang-II induced decrease in the activity of SOD and the increase in MDA levels. These results suggest that hexarelin relieves oxidative stress induced by Ang-II in H9c2 cells. Furthermore, inhibition of hexarelin-induced autophagy by 3-methyladenine, significantly ($p< 0.05$) abolished the anti-oxidative function of hexarelin. Conversely, the application of autophagy stimulator rapamycin in H9C2 hypertrophic cells significantly ($p< 0.05$) decreased Ang-II induced oxidative stress.

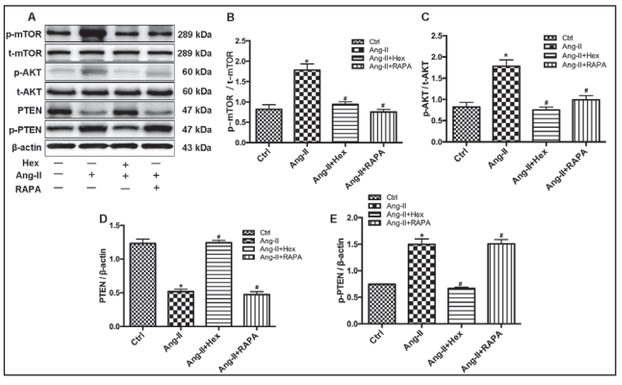

Fig. 7: Effects of hexarelin on autophagy-related signalling pathways. (A) Representative Western blotting images showing the protein expression levels of p-mTOR, p-AKT, PTEN and p-PTEN in H9C2 cells after the various group treatments. (B-E) Quantitative analysis results showing the protein expression levels of p-mTOR, p-AKT, PTEN and p-PTEN in H9C2 cells after the various group treatments (n=3). *P<0.05 versus Ctrl group; #P<0.05 versus Ang-II group.

2.10. The mTOR-signalling pathway is involved in hexarelin-induced autophagy

With the aim of dissecting molecular mechanisms and related signalling pathways underlying hexarelin-induced autophagy, we used Western blotting to explore alterations in mTOR protein expression in H9C2 cells since autophagy is known to be negatively regulated by the mTOR-signalling pathway (Ravikumar et al. 2010). Our results (Fig.7A and 7B) revealed that the phosphorylation of mTOR was markedly ($p< 0.05$) up-regulated by Ang-II but was significantly reversed ($p< 0.05$) and inhibited by hexarelin or rapamycin (an mTOR inhibitor) after H9C2 cells were treated with either Ang-II and hexarelin or with Ang-II and rapamycin. This indicates that the downregulation of mTOR phosphorylation contributes to hexarelin-induced autophagy. Since phosphatase and tensin homologue (PTEN) and AKT are involved in mTOR activity regulation, our results (Fig. 7A, 7C, 7D and 7E) also showed that compared to the Ctrl group, Ang-II also significantly ($p< 0.05$) downregulated non-phosphorylated PTEN (active form of PTEN) and up-regulated phosphorylated PTEN (inactive form of PTEN) with a corresponding increase in AKT phosphorylation. Hexarelin in the Ang-II + Hex group significantly ($p< 0.05$) reversed all these changes but rapamycin as expected had no significant effect on PTEN and AKT.

3. Discussion

According to the authors' best knowledge, this study demonstrated for the first time that hexarelin attenuates cardiomyocyte

hypertrophy by the activation of cytoprotective autophagy in H9C2 cardiomyocytes *via* the suppression of the mTOR signalling pathway.

Pathological cardiac hypertrophy, identified as a leading predictor of HF (Okin et al. 2004) and numerous cardiovascular diseases has over the years been a potential target of anti-cardiac remodelling therapy. Although numerous cardiac hypertrophic signalling pathways responsible for triggering cardiac hypertrophy exists, the secreted peptide, Ang-II in the renin-angiotensin system is a popular factor governing the pathophysiology of cardiac hypertrophy and HF.

According to recent studies, the enhancement of autophagy in the myocardium offers cardioprotection whilst the inhibition of autophagy is associated with the development of cardiac hypertrophy and HF (Orogo and Gustafsson 2015; Wu et al. 2014). Several processes occur during autophagy that finally helps in maintaining cellular homeostasis. It normally begins and characterised morphologically by the formation of double membranous cytoplasm based vesicles or vacuoles, and the subsequent engulfing of damaged organelles and proteins followed by the fusion of lysosomes to cargo-loaded autophagosomes to form autophagolysosomes. A lysosomal hydrolase that is acidic in nature then breaks down the contents engulfed in the autophagosomes. Biochemically, LC3 and Beclin-1 are popularly used autophagy specific molecular markers. Beclin-1 is a protein that reacts with Bcl-2 to promote autophagy and is also related to the inhibition of tumorigenesis and cellular proliferation (Liang et al. 1999).

LC3 can exist as LC3-I and LC3-II and are cytoplasmic and lipidated respectively. LC3-I refers to newly synthesized and cytoplasmic distributed LC3, some of which are converted to form LC3-II upon autophagy induction. Converted LC3-II forms structures that are ring-shaped and tightly bound to autophagosomes making LC3-II an autophagosome marker (Galluzzi et al. 2009). Our study proved morphologically and biochemically that Ang-II inhibits the activation of autophagy in H9C2 cells by decreasing the fluorescence intensity of autophagic LC3 protein, decreasing the fluorescence intensity of autophagosomes as shown by our Cyto-ID staining results, as well as decreasing MDC-positive autophagic vacuoles in H9C2 cells. To buttress these results, Beclin-1 and LC3 proteins were also down-regulated by Ang-II. These observations were also accompanied by the occurrence of cardiomyocyte hypertrophy demonstrated by the increase in H9C2 cell surface area and the increase in protein or mRNA expressions of ANP or BNP which are classically related to pathological cardiac hypertrophy or remodelling. These observations were in consistence with results from studies carried out by Yan et al. which demonstrated that Ang-II induced cardiac hypertrophy is accompanied by the inhibition of autophagy activation (Yan et al. 2015). Studies have shown autophagy regulatory actions of ghrelin (a known growth hormone secretagogue secreted in the stomach) in a variety of tissues (Rodriguez et al. 2012; Yuan et al. 2014) and notable among them is a study by Tong et al. (2012), which showed the cardioprotective ability of ghrelin against cardiac myocyte injury by inducing autophagy. One of our novel findings in this study showed that hexarelin (a recognized synthetic mimetic of ghrelin), reversed the inhibition of autophagy by Ang-II and increased the autophagic response in H9C2 hypertrophic cells to inhibit Ang-II induced cardiomyocyte hypertrophy. Hence, hexarelin might be a potential negative regulator of pathological cardiac hypertrophy through the enhancement of autophagy.

Another major pathological change during cardiac hypertrophy apart from cardiac cell enlargement is the apoptotic loss of cardiomyocytes (Mann et al. 2012). Previous studies have proved hexarelin's protection of cardiomyocytes from Ang-II-elicited apoptosis (Pang et al. 2004; Xu et al. 2005). Our current study also confirmed those observations. But since recent investigations have implicated the involvement of autophagy in relation to the pathogenesis of cardiomyocyte apoptosis and cardiac hypertrophy (Gottlieb and Mentzer 2010; Li et al. 2017), we became curious in finding out whether our novel finding of autophagy activation by hexarelin in this study was also involved in the hexarelin-triggered anti-apoptotic action in our H9C2 hypertrophic cells. Interestingly, our data demonstrated for the first time that inhibition of hexarelin-induced autophagy by 3-methyladenine not only abolished the anti-hypertrophic function of hexarelin, but also abrogated the protection of hexarelin against cardiomyocyte apoptosis and decline in cell viability. Conversely, the application of autophagy stimulator rapamycin in H9C2 hypertrophic cells inhibited apoptosis, increased cell viability and reduced cell size as well.

Normally, when cardiac cells require energy, adenosine diphosphate (ADP) and creatine phosphate (CP) are swiftly converted into creatine and adenosine triphosphate (ATP), so ATP is often used as a reflection of the heart's energy balance standards. Various events that occur during autophagy are known to contribute to cell survival. For instance, the recycling and regeneration of amino and fatty acids become valuable sources for the synthesis of ATP (Sciarretta et al. 2011). Other autophagic events such as the removal of impaired organelles or proteins and the maintenance of organelle function including that of the mitochondrion which is involved in energy metabolism, clearly play a vital role in cell survival (Levine and Klionsky 2004; Yang and Klionsky 2010). This also implies that when cardiac autophagy is impaired, damaged proteins and organelles such as damaged cardiac mitochondria will be accumulated which will end up triggering reactive oxygen species (ROS) production causing oxidative stress. Moreover, the induction of cardiac hypertrophy by Ang-II has been proven by numerous studies to be associated with the upsurge in mitochondrial ROS production and oxidative stress (Dai et al. 2011; Zablocki and Sadoshima 2013). Consistent with the findings in our current study, the upregulation in autophagic action of hexarelin, abrogated Ang-II-induced depletion of cellular ATP content, nullified the Ang-II-elicited increase in oxidative stress and altogether led to the increase in H9C2 cell survival and cytoprotection.

mTOR is known to be a major signalling pathway that regulates autophagy. In the presence of autophagy stimulators such as starvation or rapamycin, there is the inactivation of mTOR, which causes the formation of autophagy-regulatory complexes that signals autophagy induction (Martinet and De Meyer 2009). In contrast, increase in mTOR activation results in the attenuation of autophagy (Yu et al. 2010). Since PTEN and AKT are involved in the regulation of the mTOR signalling pathway, we therefore made an assessment of mTOR phosphorylation and its upstream signalling molecules PTEN and AKT. Our results demonstrated the suppression of mTOR phosphorylation by hexarelin in hypertrophic H9C2 cells. The mTOR upstream AKT phosphorylation was also suppressed whilst PTEN(the natural inhibitor of AKT) was upregulated.

Besides the mTOR classical pathway, so many signalling pathways known to participate in the regulation of autophagy has been reported (Criollo et al. 2010), hence more studies must be done to elucidate potential molecular mechanisms associated with hexarelin's effect on autophagy.

In summary, we propose that hexarelin plays a novel role of attenuating cardiomyocyte hypertrophy and apoptosis via an autophagy-dependent mechanism associated with the suppression of the mTOR signalling pathway. Our data provides new insights into the mechanisms underlying the possible application of hexarelin in anti-cardiac remodelling therapy.

4. Experimental

4.1. Materials

Hexarelin (C47H58N12O6) was purchased from ProSpec (East. Brunswick, NJ, USA). AngII (A9525), rapamycin (RAPA, 37094), 3-methyladenine (3-MA, M9281) and some reagents related to cell culture like the Dulbecco's modified Eagle's medium (DMEM) were all obtained from Sigma Co.(St. Louis, MO,USA). Cells in our experiment were treated with hexarelin, AngII, 3-methyladenine and rapamycin at concentrations of 1 μM, 10 mM and 100 nM respectively. Secondary antibodies conjugated with horseradish peroxidase were purchased from ZSGB-BIO (BJ, China). Anti-β-actin (#60008-1-AP) and anti-α-actin (#14395-1-AP) antibodies were obtained from Proteintech (Wuhan, China). Anti-PTEN (#ab31392) and anti-p-PTEN (#ab131107) antibodies were purchased from Abcam (Cambridge, UK). Anti-AKT (#2920), anti-p-AKT (#4060S), anti-p-mTOR (#2971S), anti-mTOR (#2983), anti-Beclin-1 (#3738S), anti-LC3A/B (#12741S) and anti-cleaved-caspase 3 (#9664) antibodies were all obtained from Cell Signaling Technology (Danvers, MA, USA). Anti-BNP (#DF6902) antibody was purchased from Affinity Biosciences (Cambridge, UK).

4.2. Cell culture

H9C2 cells were obtained from the Chinese Academy of Sciences (SH, China). DMEM high-glucose solution containing 1 % streptomycin or penicillin and 10 % fetal bovine serum (FBS)(Gibco) was used in culturing the cells. Incubation of the H9C2 cells were done in a humidified incubator of 5 % CO_2 and 95 % air atmosphere at 37 °C. After every 2 days there was a change of medium and subculturing of cells. Subsequent experiments were performed on the cells after reaching 70-80 % confluence.

4.3. Cell grouping and drug administration

The H9C2 cells were serum starved for 24 h before being treated and divided into the following eight groups: (1) Ctrl group: H9C2 cells were cultured without any other treatment for 24 h in the vehicle medium (DMEM). (2) Hex group: Hexarelin (1 μM) was added to H9C2 cells and cultured for 24 h. (3) Ang-II group: Ang-II (1 μM) was added to H9C2 cells and cultured for 24 h. (4) Ang-II + Hex group: Hexarelin (1 μM) and Ang-II (1 μM) were added to H9C2 cells and cultured for 24 h. (5) Ang-II + 3-MA group: After treating H9C2 cells with 3-MA (10 mM) for 3 h, Ang-II (1 μM) was added and further cultured for 24 h. (6) Ang-II + Hex + 3-MA group: H9C2 cells were first treated with 3-MA (10 mM) for 3 h, after which hexarelin (1 μM) and Ang-II (1 μM) were added and further cultured for 24 h. (7) Ang-II + RAPA group: H9C2 cells were first treated with rapamycin (100 nM) for 2 h, after which Ang-II (1 μM) was added and further cultured for 24 h. (8) Ang-II + Hex + RAPA group: H9C2 cells were first treated with rapamycin (100 nM) for 2 h, after which hexarelin (1 μM) and Ang-II (1 μM) were added and further cultured for 24 h.

4.4. Immunofluorescence assay

After washing H9C2 cells with phosphate-buffered saline (PBS) and fixing with 4 % paraformaldehyde on glass slides, permeabilization of the cells was achieved using 0.1% Triton X-100 (Sigma Co.). Subsequently, slides were blocked using bovine serum albumin. Specific primary antibodies (LC3 and α-actin; 1:50) were used in immunolabelling the cells at 4 °C overnight. The next day, H9C2 cells were rinsed followed by incubation with corresponding secondary antibody (fluorescein-conjugated goat anti-rabbit IgG; Rockland Immunochem. Inc., Limerick, PA). After nuclear counterstaining with DAPI, cells were finally observed with the use of fluorescence objectives equipped-microscope (Olympus IX51, Center Valley, PA).

4.5. Western blot analysis

Harvested H9C2 cells were lysed in RIPA buffer that contains PMSF. BCA Protein Assay Kit (Solarbio, BJ, China) was used to quantify the concentration of protein. Equal amounts of protein extracted were separated on SDS-polyacrylamide gels before being electrophoretically transferred to polyvinylidene fluoride membranes. After 5 % non-fat milk was used in blocking the membrane, they were incubated at 4 °C overnight with primary antibodies for BNP (1:500), β-actin (1:5000), p-PTEN (1:500), PTEN (1:500), p-mTOR (1:1000), p-AKT (1:2000), mTOR (1:1000), AKT (1:2000), Beclin-1 (1:1000), LC3A/B (1:1000) and cleaved-caspase 3 (1:1000). They were then incubated with horseradish peroxidase-conjugated secondary antibodies and the immunoreactive bands were subsequently detected with a chemiluminescent imaging analysis system. Bio-Rad Quantity One software and Bio-Rad ChemiDoc™ EQ densitometer (Bio-Rad Lab., Hercules, CA, USA) were used to quantify the immunoreactive band intensity.

4.6. Measurement of ATP concentration

The concentration of ATP in the H9C2 cells were measured using CellTiter-Glo® Luminescent Assay Kit (G7571, Promega) by strictly following the instructions of the manufacturer. The amount of ATP for each sample was evaluated using an ATP calibration curve and normalized expressed as pmol of ATP.

4.7. Quantitative real-time PCR (qRT-PCR)

Cell to cDNA kit (Bimake, Houston, TX, USA) was used in extracting total RNA from the H9C2 cells and were then reverse transcribed into cDNA using PrimeScript™ RT reagent Kit with gDNA Eraser (Takara, Shiga, Japan) by strictly following the instructions of the manufacturer. qRT-PCR was performed according to the manufacturers's instructions using SYBR Green qPCR Master Mix (Bimake, Houston, TX, USA) with a Roche LightCycler 96. The primers used were synthesized by Shanghai Sangon Biological Engineering Technology and Services Co. (Shanghai, China) and were as follows: PTEN; Forward: 5'-CCAGGACCAGAGG-AAACC-3', Reverse: 5'-GTCATTATCCGCACGCTC-3', Beclin-1; forward: 5'-CATTACTTACCA-CAGCCC-3', reverse: 5'-CATCTGTC-TGGCCAGAC-3', BNP; Forward: 5'-TGAT-TCTGCTCCTGCTTTTC-3', Reverse: 5'-GTGGATTGTTCTGGAGACTG-3', β-Actin; forward: 5'-GAGGCTC-TCTTCCAGCCTTC-3', reverse: 5'- AGGGTG-TAAAA-CGCAGCTCA-3', ANP; forward: 5'-GGCTCCTTCTCCATCACCAA-3', reverse: 5'-CGAGAGCACCTCCATCTCTC-3'. The expression of β-actin served as a control for the normalization of the expression of genes of interest. Calculation of relative gene expression was done using the 2-ΔΔCt method.

4.8. Measurement of superoxide dismutase and malondialdehyde levels

The H9C2 cultured medium from each group was obtained for measuring malondialdehyde (MDA) level and superoxide dismutase (SOD) activity using assay kits from Jiancheng Bioengineering Institute (Nanjing, China) following the manufacturer's instructions.

4.9. TUNEL assay

H9C2 cells were stained with terminal deoxynucleotidyl transferase-mediated dUTP nick end-labeling (TUNEL) assay with the use of a Cell death detection kit (Roche, Mannheim, Germany) following the instructions of the manufacturer whilst DAPI was used for nuclear counterstaining. Apoptotic index was calculated as the cell number of TUNEL-positive nuclei divided by the total number of cells across the viewed areas, and multiplied by 100.

4.10. Apoptosis assay by annexin V/propidium iodide (PI) staining

Flow cytometry was employed to detect apoptotic rate with the use of FITC annexin V apoptosis detection kit I (BD Biosciences, San Jose, CA, USA). Cold PBS was used in washing H9C2 cells before being re-suspended at a concentration of 1×10^6 cells/ml in binding buffer. After transferring 100 μl of the solution into a 5 ml culture tube, 5 μl of FITC-annexinV and 5 μl of PI were added. The cells were then incubated at room temperature in the dark for 15 min before 400 μl of binding buffer was added. Flow cytometry was used in measuring and analysing cellular fluorescence. Mod Fit LT software (Verity Software House inc, Topsham, ME, USA) was used to determine the percentage of apoptotic cells.

4.11. Cell viability assay

Cell Counting Kit-8 (CCK-8; Dojindo, Kumamoto, Japan) was used to evaluate cell viability. H9C2 cardiomyocytes were seeded at 3×10^3 cells/well in 96-well plates. After the various group treatments and conditions, 10 μl of CCK-8 was added to each well followed by 1.5 h incubation period at 37 °C. All wells were then read for optical density at 450 nm (A450) using a microplate spectrophotometer (BMG LABTECH, Offenburg, Germany).

4.12. Monodansylcadaverine (MDC) assay for autophagic vacuole visualization

MDC is a fluorescent compound identified to be a unique tracer of autophagic vacuoles (Munafó and Colombo 2001). After culturing and various group treatments of H9C2 cardiomyocytes on coverslips, they were washed thrice and fixed for 30 min with PBS and 4 % paraformaldehyde respectively. Thereafter, H9C2 cardiomyocytes were incubated with 10mmol/L of monodansylcadaverine (MDC, Sigma) in PBS for 30 min at 37 °C to label the autophagic vacuoles with MDC. Fluorescence microscopy (Olympus, XSZ-D2) was then used in analyzing the autophagic vacuoles.

4.13. Cyto-ID staining for measurement of autophagic flux

The selective staining of autophagosomes by Cyto-ID® Autophagy Detection Kit (#ENZ-51031-K200, Enzo Life Sciences) permits the evaluation of autophagic flux. H9C2 cardiomyocytes were seeded in 96-well plates and cultured at 37 °C and 5 % CO_2 in a humidified incubator. Cell density was kept below 1×10^3 cells/well. After the various group treatments, 1 μl of Cyto-ID green dye was added to the 1 ml cell culture medium and well mixed. It was then incubated for 30 min under standard cell culture conditions at 37 ºC and 5 % CO_2 in the dark. After the staining procedure, the Cyto-ID containing medium was washed away and a fluorescence microplate reader was used to detect the fluorescence intensity as a reflection of autophagic flux level. A confocal laser scanning microscope (Nikon, Tokyo, Japan) was then used to observe the cells.

4.14. Statistical analysis

Statistical software SPSS 21.0 for windows was used for the statistical analysis. All data were presented as mean±standard error of the mean (SEM). One-way analysis of variance (ANOVA) followed by the Student-Newman-Keuls test was used for statistical analyses of three or more groups. Statistically significant differences between two groups were determined by conducting the Student t-test. P-values that were < 0.05 were considered to be statistically significant. GraphPad Prism was used for curve fitting.

Acknowledgement: This research was funded by the Natural Science Foundation of China (81370342).

Declaration of interest: The authors report no conflicts of interest. The authors alone are responsible for the content and writing of this paper.

References

Biederbick A, Kern HF, Elsässer H (1995) Monodansylcadaverine (MDC) is a specific in vivo marker for autophagic vacuoles Eur J Cell Biol 66: 3-14.

Bisping E, Wakula P, Poteser M, Heinzel FR (2014) Targeting cardiac hypertrophy: toward a causal heart failure therapy. J Cardiovasc Pharmacol 64: 293-305.

Criollo A, Senovilla L, Authier H, Maiuri MC, Morselli E, Vitale I, Kepp O, Tasdemir E, Galluzzi L, Shen S (2010) The IKK complex contributes to the induction of autophagy. EMBO J 29: 619-631.

Dai DF, Johnson SC, Villarin JJ, Chin MT, Nieves-Cintron M, Chen T, Marcinek DJ, Dorn GW, 2nd, Kang YJ, Prolla TA, Santana LF, Rabinovitch PS (2011) Mitochondrial oxidative stress mediates angiotensin II-induced cardiac hypertrophy and Galphaq overexpression-induced heart failure. Circ Res 108: 837-846.

De Gennaro-Colonna V, Rossoni G, Cocchi D, Rigamonti A, Berti F, Muller E (2000) Endocrine, metabolic and cardioprotective effects of hexarelin in obese Zucker rats. J Endocrinol 166: 529-536.

Filigheddu N, Fubini A, Baldanzi G, Cutrupi S, Ghè C, Catapano F, Broglio F, Bosia A, Papotti M, Muccioli G (2001) Hexarelin protects H9c2 cardiomyocytes from doxorubicin-induced cell death. Endocrine 14: 113-119.

Galluzzi L, Aaronson S, Abrams J, Alnemri E, Andrews D, Baehrecke E, Bazan N, Blagosklonny M, Blomgren K, Borner C (2009) Guidelines for the use and interpretation of assays for monitoring cell death in higher eukaryotes Cell Death Differ 16: 1093.

Gottlieb RA, Mentzer Jr RM (2010) Autophagy during cardiac stress: joys and frustrations of autophagy. Annu Rev Physiol 72: 45-59.

Heineke J, Molkentin JD (2006) Regulation of cardiac hypertrophy by intracellular signalling pathways. Nature Rev Mol Cell Biol 7: 589-600.

Hill JA, Olson EN (2008) Cardiac plasticity. N Engl J Med 358: 1370-1380.

Katz AM (2008) The "modern" view of heart failure: how did we get here? Circ Heart Fail 1: 63-71.

Koitabashi N, Kass DA (2012) Reverse remodeling in heart failure—mechanisms and therapeutic opportunities. Nature Rev Cardiol 9: 147-157.

Levine B, Klionsky DJ (2004) Development by self-digestion: molecular mechanisms and biological functions of autophagy. Dev Cell 6: 463-477.

Li J, Li Y, Zhang Y, Hu D, Gao Y, Shang H, Xing Y (2017) The inhibitory effect of WenxinKeli on H9C2 cardiomyocytes hypertrophy induced by angiotensin II through regulating autophagy activity. Oxid Med Cell Longev 2017: 7042872.

Liang XH, Jackson S, Seaman M, Brown K, Kempkes B, Hibshoosh H, Levine B (1999) Induction of autophagy and inhibition of tumorigenesis by beclin 1 Nature 402: 672-676.

Mann DL, Barger PM, Burkhoff D (2012) Myocardial recovery and the failing heart: myth, magic, or molecular target? J Am Coll Cardiol 60: 2465-2472.

Mao Y, Tokudome T, Kishimoto I (2014) The cardiovascular action of hexarelin. J Geriatr Cardiol 11: 253-258.

Mao Y, Tokudome T, Kishimoto I, Otani K, Hosoda H, Nagai C, Minamino N, Miyazato M, Kangawa K (2013) Hexarelin treatment in male ghrelin knockout mice after myocardial infarction. Endocrinology 154: 3847-3854.

Martinet W, De Meyer GR (2009) Autophagy in atherosclerosis: a cell survival and death phenomenon with therapeutic potential. Circ Res 104: 304-317.

Mizushima N, Komatsu M (2011) Autophagy: renovation of cells and tissues. Cell 147: 728-741.

Mudd JO, Kass DA (2008) Tackling heart failure in the twenty-first century. Nature 451: 919-928.

Munafó DB, Colombo MI (2001) A novel assay to study autophagy: regulation of autophagosome vacuole size by amino acid deprivation. J Cell Sci 114: 3619-3629.

Nakai A, Yamaguchi O, Takeda T, Higuchi Y, Hikoso S, Taniike M, Omiya S, Mizote I, Matsumura Y, Asahi M (2007) The role of autophagy in cardiomyocytes in the basal state and in response to hemodynamic stress. Nat. Med. 13: 619-624.

Okin PM, Devereux RB, Harris KE, Jern S, Kjeldsen SE, Julius S, Edelman JM, Dahlöf B (2007) Regression of electrocardiographic left ventricular hypertrophy is associated with less hospitalization for heart failure in hypertensive patients. Ann Intern Med 147: 311-319.

Okin PM, Devereux RB, Jern S, Kjeldsen SE, Julius S, Nieminen MS, Snapinn S, Harris KE, Aurup P, Edelman JM (2004) Regression of electrocardiographic left ventricular hypertrophy during antihypertensive treatment and the prediction of major cardiovascular events. JAMA 292: 2343-2349.

Orogo AM, Gustafsson ÅB (2015) Therapeutic targeting of autophagy: potential and concerns in treating cardiovascular disease. Circ Res 116: 489-503.

Pang J-J, Xu R-K, Xu X-B, Cao J-M, Ni C, Zhu W-L, Asotra K, Chen M-C, Chen C (2004) Hexarelin protects rat cardiomyocytes from angiotensin II-induced apoptosis in vitro. Am J Physiol Heart Circ Physiol 286: H1063-H1069.

Ravikumar B, Sarkar S, Davies JE, Futter M, Garcia-Arencibia M, Green-Thompson ZW, Jimenez-Sanchez M, Korolchuk VI, Lichtenberg M, Luo S (2010) Regulation of mammalian autophagy in physiology and pathophysiology. Physiol Rev 90: 1383-1435.

Rodriguez A, Gomez-Ambrosi J, Catalan V, Rotellar F, Valenti V, Silva C, Mugueta C, Pulido M, Vázquez R, Salvador J (2012) The ghrelin O-acyltransferase–ghrelin system reduces TNF-α-induced apoptosis and autophagy in human visceral adipocytes. Diabetologia 55: 3038-3050.

Sciarretta S, Hariharan N, Monden Y, Zablocki D, Sadoshima J (2011) Is autophagy in response to ischemia and reperfusion protective or detrimental for the heart? Pediatr Cardiol 32: 275-281.

Stewart S, MacIntyre K, Hole DJ, Capewell S, McMurray JJ (2001) More 'malignant'than cancer? Five-year survival following a first admission for heart failure. Eur J Heart Fail 3: 315-322.

Tong X-X, Wu D, Wang X, Chen H-L, Chen J-X, Wang X-X, Wang X-L, Gan L, Guo Z-Y, Shi G-X (2012) Ghrelin protects against cobalt chloride-induced hypoxic injury in cardiac H9c2 cells by inhibiting oxidative stress and inducing autophagy. Peptides 38: 217-227.

Wu X, He L, Chen F, He X, Cai Y, Zhang G, Yi Q, He M, Luo J (2014) Impaired autophagy contributes to adverse cardiac remodeling in acute myocardial infarction PLoS One 9: e112891.

Xu X, Pang J, Yin H, Li M, Hao W, Chen C, Cao J-M (2007) Hexarelin suppresses cardiac fibroblast proliferation and collagen synthesis in rat. Am J Physiol Heart Circ Physiol 293: H2952-H2958.

Xu X-B, Pang J-J, Cao J-M, Ni C, Xu R-K, Peng X-Z, Yu X-X, Guo S, Chen M-C, Chen C (2005) GH-releasing peptides improve cardiac dysfunction and cachexia and suppress stress-related hormones and cardiomyocyte apoptosis in rats with heart failure. Am J Physiol Heart Circ Physiol 289: H1643-H1651.

Yan W, Guo L, Zhang Q, Sun W, O'rourke S, Liu K, Sun C (2015) Chronic blockade of class I PI3-kinase attenuates Ang II-induced cardiac hypertrophy and autophagic alteration. Eur Rev Med Pharmacol Sci 19: 772-783.

Yang Z, Klionsky DJ (2010) Eaten alive: a history of macroautophagy. Nat Cell Biol 12: 814-822.

Yu L, McPhee CK, Zheng L, Mardones GA, Rong Y, Peng J, Mi N, Zhao Y, Liu Z, Wan F Hailey DW, Oorschot V, Klumperman J, Baehrecke EH, Lenardo MJ (2010) Termination of autophagy and reformation of lysosomes regulated by mTOR. Nature 465: 942-946.

Yuan H, Niu Y, Liu X, Fu L (2014) Exercise increases the binding of MEF 2A to the Cpt1b promoter in mouse skeletal muscle. Acta Physiol 212: 283-292.

Zablocki D, Sadoshima J (2013) Angiotensin II and oxidative stress in the failing heart. Antioxid Redox Signal 19: 1095-1109.